Molecular Beam Deposition of DNA Nanometer Films

Joshua A. Hagen,[†] Wei-Xin Li,[†] Hans Spaeth,[†] James G. Grote,[‡] and Andrew J. Steckl*,[†]

Nanoelectronics Laboratory, University of Cincinnati, Cincinnati, Ohio 45221-0030, and U.S. Air Force Research Laboratory, Dayton, Ohio 45324

ABSTRACT

The development of novel photonic devices which incorporate biological materials is strongly tied to the development of thin film forming processes. Solution-based ("wet") processes when used with biomaterials in device fabrication suffer from dissolution of underlying layers, incompatibility with clean environment, inconsistent film properties, etc. We have investigated ultra-high-vacuum molecular beam deposition of surfactant-modified deoxyribonucleic acid (DNA). We have obtained effective deposition rates of ∼0.1–1 Å/s, enabling reproducible and controllable deposition of nanometer-scale films.

Interest is continuing to increase[1−5] rapidly in the optical and electronic properties of DNA and other biopolymers and in related device applications. Usually, reports on these properties are either based on relatively thick films obtained by "wet" processes (such as spin-coating) techniques[6] or based on heroic efforts with single molecules.[7,8] In this paper, we report on the properties of nanometer-scale surfactant-modified DNA thin films formed by molecular beam deposition[9−11] (MBD). In general, polymers, unlike small molecule organic materials, do not usually lend themselves to MBD since their high molecular weight results in very low vapor pressures (and negligible deposition) up to their decomposition temperature. However, we have found that several types of complexed DNA can be deposited by MBD with subnanometer thin film control, thus opening the door to its incorporation in nanoscale devices. MBD is a thermal evaporation technique widely utilized in the fabrication of photonic devices based on compound semiconductors, where it is commonly known as molecular beam epitaxy (MBE) since the thin films have an epitaxial relationship to the substrate on which they are grown. This deposition technique takes place under high vacuum conditions, which allows the formation of a molecular beam (with a minimum of scattering) and results in deposition rates of the order of 1 Å/s for atomic or small molecule materials. The small furnace (or effusion cell) that holds the material to be evaporated is connected to the high vacuum chamber. The deposition rate is controllable with high precision over a wide range by adjusting the temperature of the effusion cell containing the material. An MBD chamber with several cells can be utilized for the sequential deposition of multiple materials for the formation of complex device structures. This in situ "dry" process in a high vacuum environment prevents the generation of defects by contamination of the materials or by particulate deposition from the environment, both of which can occur during wet processing.

We have previously reported[12] on the first use of spin-coated DNA complex films as electron "blocking" layers (EBL) in organic light-emitting devices (OLEDs), showing significant enhancement in both luminance and device efficiency over conventional device structures. In this paper, we report on the properties of nanometer-thin DNA-based films by the MBD technique.

We have used DNA which was processed[6,13] from salmon sperm (saDNA). The saDNA was rendered water insoluble (but soluble in polar organic solvents) by reaction with a cationic surfactant (cetyltrimethylammonium, CTMA). The resulting DNA−CTMA complex was the primary material deposited by MBD. We have also investigated the MBD deposition of a DNA−Eu complex, which is formed from the reaction of aqueous DNA solutions with a Eu pigment. Figure 1 shows the MBD chamber pressure and deposition rate as a function of the effusion cell temperature for DNA−CTMA and DNA−Eu complexes. The deposition pressures for both DNA−CTMA and DNA−Eu increase with cell temperature. As shown in Figure 1a, at relatively low temperatures (∼130−160 °C) the DNA−Eu complex pressure was an order of magnitude lower than that of the DNA−CTMA but increased more rapidly with temperature. In the 160−170 °C temperature range, the pressure increased rapidly for both DNA complexes. Starting at ∼170 °C, the

* Corresponding author. E-mail: a.steckl@uc.edu.
† Nanoelectronics Laboratory, University of Cincinnati.
‡ U.S. Air Force Research Laboratory.
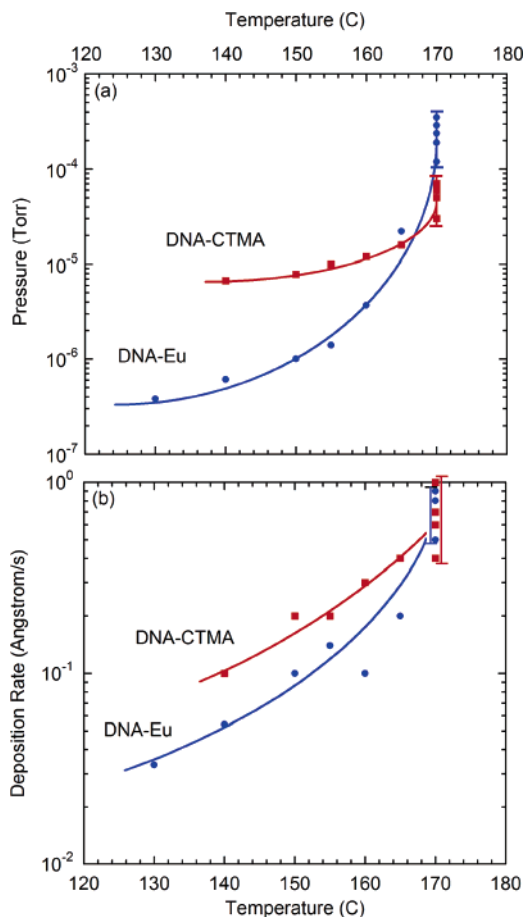
Figure 1. Effect of effusion cell temperature on DNA−CTMA and DNA−Eu complexes: (a) vapor pressure in the deposition chamber as a function of cell temperature; (b) thin film deposition rate as a function of cell temperature.

vapor pressure produced by the two DNA complexes tended to become somewhat unstable with time, as indicated in Figure 1a by the multiple data points at that temperature. To obtain reproducible thin film deposition characteristics, the DNA cell temperature was maintained between 155 and 170 °C, well below the 225 °C degradation point obtained by thermogravimetric analysis of DNA−CTMA (see Supporting Information). Consistently with their vapor pressures, the DNA−CTMA deposition rate was generally higher than that of DNA−Eu, as shown in Figure 1b. At cell temperatures in the 150−160 °C range, the DNA-CTMA deposition rate was in the 0.2−0.3 Å/s range and the DNA−Eu deposition rate was ∼0.1 Å/s. At the cell temperature of 170 °C, the deposition rates for both DNA complexes were in the same ∼0.5−1 Å/s range. Clearly, these deposition rates allow for the formation of nanometer DNA films with excellent thickness control.

The DNA films obtained by MBD displayed a very smooth and uniform surface. As seen in the photomicrograph contained in Figure 2, the DNA−CTMA film surface is featureless. This was obtained from a relatively thick 250 nm film deposited at an effusion cell temperature of 180 °C. The insert shows an optical photograph of the MBD DNA−CTMA film on a glass substrate. The yellowish background of the photograph was selected in order to yield sufficient
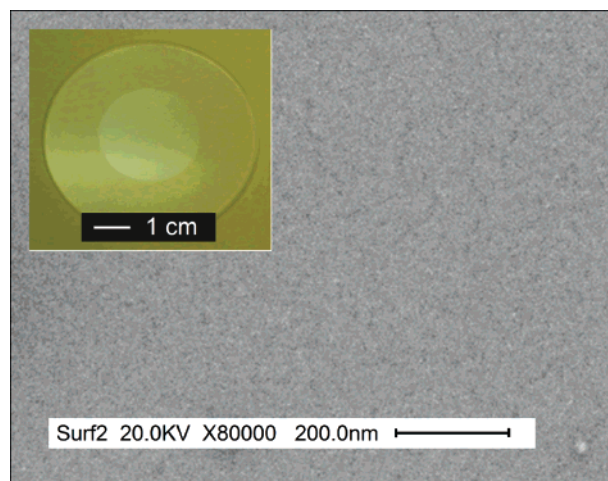

Figure 2. DNA−CTMA thin film surface morphology. Electron micrograph of 250 nm DNA−CTMA film surface. Inset: Optical photograph of patterned DNA film on 2 in. quartz substrate.
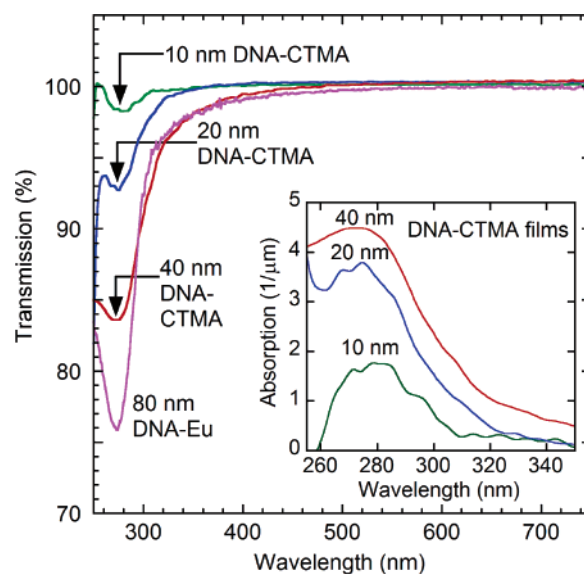
Figure 3. Optical properties of DNA−CTMA and DNA−Eu thin films. Transmission versus wavelength for 10, 20, 40 nm DNA−CTMA films and an 80 nm DNA:Eu film. Inset: Absorption coefficient versus wavelength for DNA−CTMA films.

contrast between the film and the glass substrate. The resulting film is optically transparent and exhibits a pinhole-free smooth surface.

The optical transmission properties of MBD DNA films are shown in Figure 3. Transmission spectra for 10, 20, and 40 nm DNA−CTMA films and an 80 nm DNA−Eu film all exhibit an ultraviolet (UV) absorption peak at ∼275 nm. Thicker solution-processed DNA−CTMA films obtained from the same saDNA source have a ∼260 nm UV absorption peak,[2] which is the wavelength normally associated[14,15] with DNA molecules. It is not yet clear what is the reason for the difference in absorption peak wavelength between the MBD DNA−CTMA and the solution-processed DNA−CTMA. It is interesting to point out that a slight blue shift in peak wavelength with increasing film thickness is evident for the MBD DNA−CTMA films. In the visible range from 450 to 750 nm there is very little absorption even
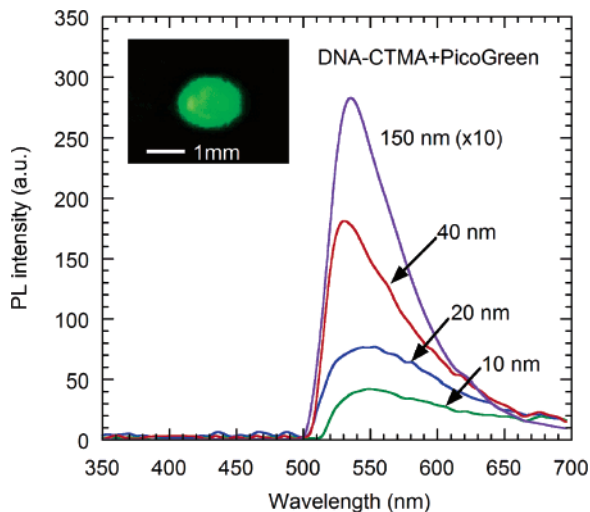
Figure 4. Effect of DNA-intercalating fluorescent dye. Photoluminescence spectra of DNA−CTMA films of different thicknesses, stained with Picogreen dye and excited at 488 nm. Inset: Photograph of PL emission from DNA−CTMA + Picogreen region pumped at 488 nm.

Figure 5. Optical emission from MBD film of DNA reacted with Eu complex under 325 nm excitation. Photoluminescence spectrum DNA−Eu film. Inset: Optical photograph of Eu PL emission.

for the 80 nm DNA−Eu film. The transmission/absorption spectra of the MBD DNA films are a close match to solution-based DNA material. As expected, the transmission at 275 nm decreases with increasing film thickness. However, as shown in the insert in Figure 3, the peak absorption coefficient at 275−280 nm for several DNA−CTMA films is not constant but rather increases with film thickness, ranging from ∼1.8 μm^{-1} for the 10 nm film to 4.5 μm^{-1} for the 20 nm film. This indicates that the structure of the very thin nanometer DNA films may be different from that of thicker films.

We have used a double strand DNA-specific fluorescent dye (Picogreen) to provide additional confirmation that the MBD films preserve the DNA structure. Picogreen works as a DNA identifier[16] as it emits characteristic green emission only when it intercalates within the DNA double helix structure. Figure 4 shows the photoluminescence (PL) spectra of several DNA−CTMA films with different thickness stained with Picogreen dye. One drop of methanol together with one drop of Picogreen solution was successively dispensed onto each DNA−CTMA film. Methanol was utilized to partially dissolve the DNA film so that the DNA molecules are able to interact with the Picogreen dye. The droplet was then optically pumped with an Ar laser at 488 nm. The intensity of the green emission peaking at ∼540 nm increased with the film thickness, as more DNA is available for Picogreen intercalation into the DNA double helix. The insert in Figure 4 shows a photograph of the PL emission from a Picogreen-stained DNA−CTMA film excited with the Ar laser. The characteristic green emission from Picogreen dye confirms the existence of DNA molecules since Picogreen itself does not luminesce in the absence of DNA. Furthermore, this confirms that the DNA has not undergone denaturing (or other major structural changes) which would prevent Picogreen intercalation.

High molecular weight saDNA in aqueous solution was also complexed with a europium pigment, and the resulting
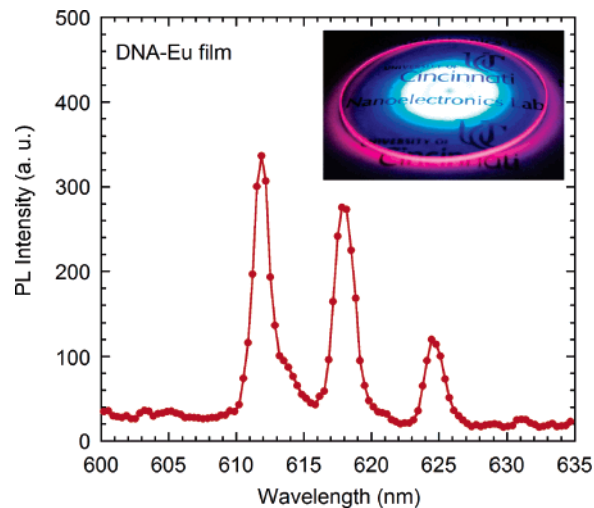
material was deposited by MBD. Figure 5 shows the PL spectrum of a DNA−Eu film excited at 325 nm with a HeCd laser. Characteristic[17−19] sharp emission lines at 612, 618, and 625 nm were observed due to the Eu^{3+} 4f inner shell transitions. The insert in Figure 5 shows an optical photograph of a DNA−Eu film on a glass substrate excited at 325 nm. The central white spot resulted from the response of the background white paper to the UV excitation of the HeCd laser, while the strong red emission at the glass substrate edge resulted from the waveguided Eu PL emission. Excitation of a DNA−Eu film stained with Picogreen at 488 nm with the Ar laser produces strong green emission similar to the case of the DNA−CTMA films, providing additional evidence that the DNA double helix structure is preserved in DNA−Eu MBD films.

Organic light-emitting devices (OLEDs) incorporating MBD DNA−CTMA films (so-called BiOLEDs) were fabricated to evaluate the effectiveness of MBD DNA films in a device structure. The baseline OLED device structure consists of ITO/PEDOT:PSS (50 nm)/NPB (30 nm)/Alq_3 (40 nm)/BCP (20 nm)/Alq_3 (10 nm)/Li:Al, while the BiOLED has an additional DNA−CTMA layer (15 nm) located between the PEDOT and NPB layers in order to control the electron flow by introducing the blocking LUMO (lowest unoccupied molecular orbital) level of the DNA layer (see Supporting Information for definitions of compounds used in the device). The effect of blocking electron flow is to enhance the probability of radiative electron−hole recombination,[20,21] leading to increased device luminous efficiency and luminance.

The energy level diagram of the BioLED was previously reported.[12] Indium tin oxide (ITO) serves as the anode; PEDOT:PSS functions as a hole injection layer; DNA−CTMA is an electron blocking layer (EBL); NPB is used as hole transport layer; Alq_3 is used for both the electron transport layer and the emitter layer; BCP functions as a hole blocking layer; LiF:Al is a low work function cathode.
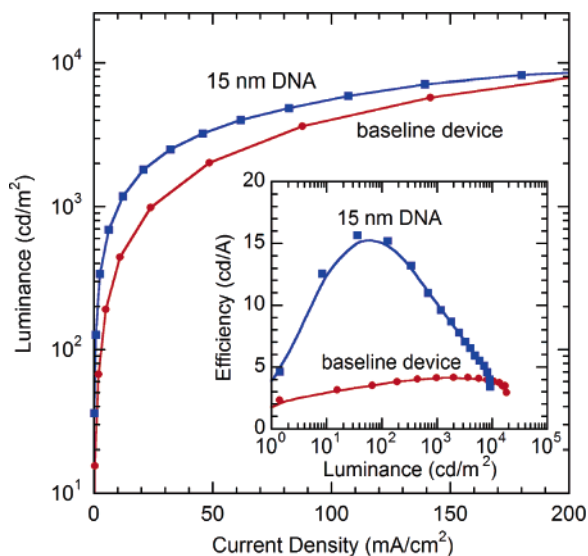
Figure 6. DNA−CTMA photonic device performance. Luminance versus current density for a BioLED with a 15 nm DNA−CTMA film. Inset: Efficiency vs luminance for BioLED (with DNA) and baseline (no DNA) devices.

The luminance−current density (L-J) characteristic of a BiOLED with a 15 nm DNA−CTMA film is shown in Figure 6. The L-J of a baseline device (without the DNA layer) is also shown for comparison. The insertion of the DNA EBL leads to consistently higher luminance over the entire range of current densities, with a ∼2× improvement at the lower values of current density. The Figure 6 insert shows the luminous efficiency as a function of luminance for the same two devices. The maximum efficiency of the BiOLED device is higher by a factor of ∼5× over the baseline device. The maximum luminous efficiency reaches ∼16 cd/A (equivalent to ∼5% external quantum efficiency) at a luminance of ∼50 cd/m². This quantum efficiency accounts for nearly 100% singlet recombination efficiency within the emissive layer and is the highest value reported for fluorescent emission.

Photonic and electronic devices which utilize polymeric materials have traditionally employed solution-based techniques for thin film formation: spin-coating, dip-coating, inkjet printing, etc. Dry processing using physical or chemical vapor deposition has been restricted to small organic molecules. Solution-based approaches have been demonstrated to be capable of producing highly uniform layers with thickness ranging from several micrometers down to several tens of nanometers. Scaling the thickness of solution-deposited films to less than 10 nm with subnanometer control and low pinhole count will be a challenging task. Furthermore, solution-based polymer deposition has an inherent limitation in fabricating thin film device structures simply because the solution to be coated could dissolve the existing underlying thin film structure. By comparison, the dry MBD method avoids using any solvent and, thus, can be readily deposited onto almost any surface. Furthermore, MBD enables monolayer control over the growth of organic thin films with high chemical purity. In addition, since MBD is a high vacuum technique it usually incorporates powerful in situ diagnostics (such as residual gas analysis, reflection high-energy electron diffraction) to study the film properties during growth.

Our results show that despite the large molecular size of the starting DNA material, high optical quality, pinhole-free DNA thin films were readily obtained using the MBD approach. The evaporated DNA−CTMA films were found to have a much lower electrical resistance (∼10^5 Ω cm) than that of solution-based (spin-coated) DNA films (∼10^{10} Ω cm, see Supporting Information), suggesting that the DNA in the MBD films has a lower molecular weight than that in the spin-coated films. This may be explained by considering that smaller DNA strands (oligomers) probably have a higher vapor pressure than larger molecules, thus being first (or primarily) evaporated and contributing a disproportionate amount in MBD DNA−CTMA films compared to spin-coated DNA−CTMA films from the same starting batch. Another difference between the two processes that may play a role is the fact that in MBD many impurities (such as water molecules, nitrogen, oxygen, etc.) are eliminated from the starting material by outgassing prior to deposition. The size distribution of the evaporated DNA molecules is currently under investigation. The mechanical properties of MBD films were also found to be superior to the spin-coated counterparts. For example, the physical adhesion between DNA−CTMA films and glass substrates is much stronger for the MBD films than that for the spin-coated films.

Finally, from a device point of view, the superior device output efficiency of the MBD BiOLED (16 cd/A) over the spin-coated BiOLED[12] (8 cd/A) and the no-DNA baseline device (3 cd/A) further indicates the high quality of DNA−CTMA films deposited by the MBD approach. The nearly 100% singlet recombination efficiency makes the MBD DNA material a very attractive candidate as a high efficiency EBL in the OLED field.[22] This is particularly important for achieving high efficiency blue emitting devices,[23−26] where electron−hole current balance is a major concern. DNA has also been found to be able to act as a host material which enhances the intensity of dye emission[5,27] by intercalating dye molecules within its double helix structure which resulted in reduced concentration quenching. The strong saturated red emission from DNA−Eu films indicates the great potential of the MBD approach for evaporated DNA−dye complexes to serve as the OLED emissive layer, thus obtaining more efficient devices.

In conclusion, the MBD-based approach to biopolymer thin film deposition could provide a very attractive approach for the integration of biomaterials in photonic and electronic devices, specifically those requiring nanometer dimensions.

Supporting Information Available: Additional information about thermogravimetric analysis, film resistivity as a function of DNA molecular weight, and materials used in

the device structure. This material is available free of charge via the Internet at http://pubs.acs.org.

References

(1) Stroscio, M. A.; Dutta, M. *Proc. IEEE* **2005**, *93*, 1772−1783.
(2) Wang, L.; Yoshida, J.; Ogata, N. *Chem. Mater.* **2001**, *13*, 1273−1281.
(3) Porath, D.; Bezryadin, B.; Vries, S. d.; Dekker, C. *Nature* **2000**, *403*, 635−638.
(4) Okahata, Y.; Kobayashi, T.; Tanaka, K.; Shimomura, M. *J. Am. Chem. Soc.* **1998**, *120*, 6165−6166.
(5) Grote, J. G.; Hagen, J. A.; Zetts, J. S.; Nelson, R. L.; Diggs, D. E.; Stone, M. O.; Yaney, P. P.; Heckman, E.; Zhang, C.; Steier, W. H.; Jen, A. K.-Y.; Dalton, L. R.; Ogata, N.; Curley, M. J.; Clarson, S. J.; Hopkins, F. K. *J. Phys. Chem. B* **2004**, *108*, 8584−8591.
(6) Heckman, E.; Hagen, J.; Yaney, P.; Grote, J.; Hopkins, F. K. *Appl. Phys. Lett.* **2005**, *87*, 211115.
(7) Cai, L.; Tabata, H.; Kawai, T. *Appl. Phys. Lett.* **2000**, *77*, 3105−3107.
(8) Fink, H.; Schonenberger, C. *Nature* **1999**, *398*, 407−410.
(9) So, F. F.; Forrest, S. R.; Shi, Y. Q.; Steier, W. H. *Appl. Phys. Lett.* **1990**, *56*, 674−676.
(10) Hermann, M. A.; Sitter, H. *Molecular Beam Epitaxy*; Springer: Berlin, 1996.
(11) Forrest, S. R. *Chem. Rev.* **1997**, *97*, 1793−1896.
(12) Hagen, J. A.; Li, W. X.; Steckl, A. J.; Grote, J. *Appl. Phys. Lett.* **2006**, *88*, 171109.
(13) Tanaka, K.; Okahata, Y. *J. Am. Chem. Soc.* **1996**, *118*, 10679−10683.
(14) LaMontagne, M. G.; F. C. Michel, J.; Holden, P. A.; Reddy, C. A. *J. Microbiol. Methods* **2002**, *49*, 255−264.
(15) Glasel, J. A. *Biotechniques* **1995**, *18*, 62−63.
(16) Singer, V. L.; Jones, L. J.; Yue, S. T.; Haugland, R. P. *Anal. Biochem.* **1997**, *249*, 228−238.
(17) Zhong, G.; Kima, K.; Jin, J. *Synth. Met.* **2002**, *129*, 193−198.
(18) Fu, Y. J.; Wong, T. K. S.; Yan, Y. K.; Hu, X. *J. Alloys Compd.* **2003**, *358*, 235−244.
(19) Male, N.; Salata, O.; Christou, V. *Synth. Met.* **2002**, *126*, 7−10.
(20) Naka, S.; Okada, H.; Onnagawa, H.; Yamaguchi, Y.; Tsutsui, T. *Synth. Met.* **2000**, *111−112*, 331−333.
(21) Li, W. X.; Jones, R.; Allen, S.; Heikenfeld, J.; Steckl, A. J. *J. Disp. Technol.* **2006**, *2*, 143−152.
(22) He, G.; Pleiffer, M.; Leo, K.; Hofmann, M.; Birnstock, J.; Pudzich, R.; Salbeck, J. *Appl. Phys. Lett.* **2004**, *85*, 3911−3913.
(23) Zhang, X.; Jiang, C.; Mo, Y.; Xu, Y.; Shi, H.; Cao, Y. *Appl. Phys. Lett.* **2006**, *88*, 051116-05111.6-3.
(24) Yeh, S.-J.; Wu, M.-F.; Chen, C.-T.; Song, Y.-H.; Chi, Y.; Ho, M.-H.; Hsu, S.-F.; Chen, C. H. *Adv. Mater.* **2005**, *17*, 285−289.
(25) Tokito, S.; Tsuzuki, T.; Sato, F.; Iijima, T. *Curr. Appl. Phys.* **2005**, *5*, 331−336.
(26) Tokito, S.; Iijima, T.; Suzuri, Y.; Kita, H.; Tsuzuki, T.; Sato, F. *Appl. Phys. Lett.* **2003**, *83*, 569−571.
(27) Ci, Y.-X.; Li, Y.; Liu, X.-J. *Anal. Chem.* **1995**, *67*, 1785−1788.

NL062342U

Thermal Stability of DNA-CTMA Thin Films

One of the biggest concerns with using organic materials in optoelectronic device applications is temperature stability of the materials. This is the most prevalent difference between organic and inorganic materials, with the latter being able to withstand high temperatures, generally anywhere from 800°C to 1400°C. Some organic materials can begin to degrade at only 100°C, which obviously would preclude them from usage in a device. The thermal stability of solid DNA-CTMA was studied using thermogravimetric analysis (TGA), which measures the weight loss of a material with increasing temperature. Once dramatic weight loss occurs in an organic material, molecular degradation has begun. As shown in the figure below, DNA-CTMA is stable until ~225°C, which makes it a thermally viable material for optoelectronic device applications.
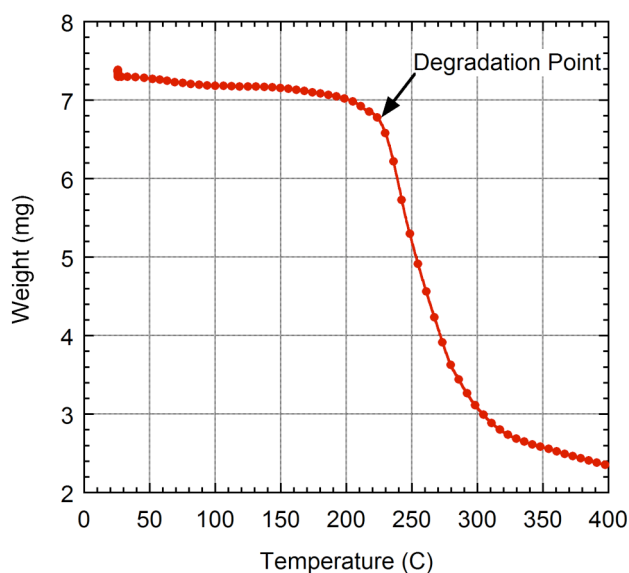

Fig. 1 (supplemental) Weight of DNA-CTMA material as a function of temperature.

DNA molecular weight

The molecular weight (MW) of the DNA starting material is typically ~ 8MDa. The DNA MW can be adjusted by mechanical or acoustic shearing in order to reduce its electrical resistivity. For the MBD of DNA-CTMA films and associated BioLED fabrication, we have used DNA with molecular weight of 145kDa, which resulted in DNA-CTMA *spin-coated* thin film resistivity is ~1.5×10^{10} Ω-cm, as shown in the figure below.
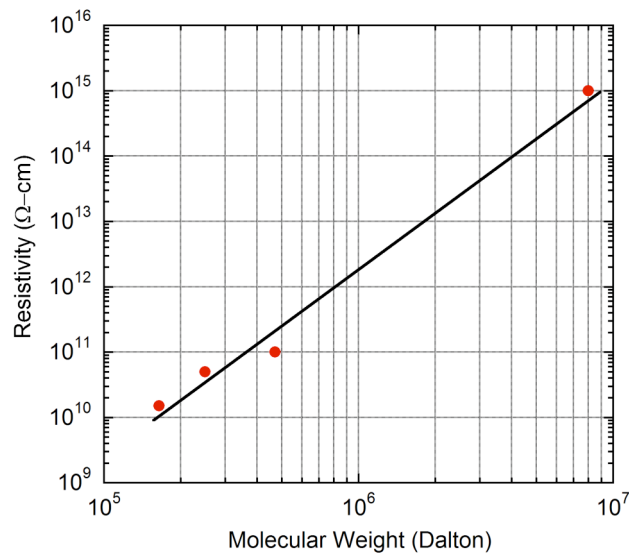

Fig. 2 (supplemental) Resistivity of DNA-CTMA spin-coated thin films as a function of DNA molecular weight.

For the MBD of DNA-Eu films, we have used aqueous solutions of the starting DNA material.

Experimental procedures

The salmon DNA is mechanically treated to reduce its molecular weight [13]. The saDNA used in these experiments has an average molecular weight of 145kDa which corresponds to 220 base pairs or a molecular length of 75 nm. DNA is converted to a

DNA-CTMA (cetyltrimethylammonium) complex by a cationic surfactant reaction, resulting in a compound that is soluble in organic solvents but insoluble in water. A DNA-Eu complex is obtained by mixing the saDNA water solution with a Eu complex methanol solution.

PEDOT [poly(3,4-ethylenedioxythiophene) doped with poly(4-styrenesulfonate)] was obtained from H. C. Stark (Baytron P™). NPB [(N,N'-bis(naphthalen-1-yl)-N,N'-bis(phenyl)benzidine)], Alq$_3$ [tris-(8-hydroxyquinoline) aluminum] and BCP [2,9-Dimethyl-4,7-diphenyl-1,10-phenanthroline] were purchased from H. W. Sands and used without any further purification.

DNA complexes were maintained at ~ 80 °C for 10 to 12 hr in a vacuum oven to drive off volatile impurities which resulted from the formation reaction prior to introduction into the ultra-high vacuum molecular beam deposition (MBD) system (from SVT Associates). Both DNA-CTMA and DNA-Eu materials were deposited at a base pressure of ~ 1×10^{-8} Torr. The deposition rate is calibrated using a crystal monitor and controlled by the cell temperature. For OLED and BioLED fabrication PEDOT/PSS (50 nm) is spin deposited onto the ITO (80 nm) anode, while the remaining organic layers were evaporated in the MBD system with the deposition rate controlled at ~2 Å/s. LiF is evaporated at a rate of 1 Å/s and Al is evaporated at 7 Å/s. The active device area is 2×2 mm^2. The substrates were cleaned using an acetone/methanol ultrasonic bath and subsequently rinsed in deionized water.

The optical transmission spectrum is obtained with a Perkin Elmer spectrometer. The absorption coefficient is then calculated from its transmission according to the film thickness. PL spectra of Picogreen™-stained DNA films and DNA-Eu films

were measured with an Ocean Optics SD 2000 fiber optic spectrometer. The dsDNA-specific Picogreen™ dye was purchased from Invitrogen Molecular Probes.

OLEDs were tested at room temperature without any encapsulation. The current density-voltage (J-V) characteristics were obtained with an HP-6634B DC power source controlled by a LabView™ program. The luminance is obtained through the transparent glass substrate with a Minolta CS-100 luminance meter. The external quantum efficiency is calculated from the luminous efficiency based on the assumption that the emission has a lambertian pattern and the emission spectrum is angle independent.